Appendix B: Cross-Frame Design Example (Straight Bridge)

Introduction

This document follows the Steel Bridge Design Handbook (SBDH) Design Example 2A: Two-Span Continuous Straight Composite Steel I-Girder Bridge (Barth 2015). In that example, girder design and detailing is evaluated extensively. Based on the findings and results of NCHRP Project 12-113, the calculations presented herein expand on SBDH Design Example 2A. In general, the calculations follow AASHTO *LRFD* 9th Edition Specifications (2020), or as modified based on the recommendations of NCHRP 12-113. These proposed recommendations are discussed and illustrated with sample calculations. For clarity, AASHTO *LRFD* article numbers are simply referred to as Article 4.6.3 (as an example) herein.

This document focuses on three major components of cross-frame design: (i) analysis techniques, (ii) combining force effects including stability bracing requirements, and (iii) estimating the capacity/resistance for all relevant limit states. Following this brief introductory section and an overview of pertinent AASHTO *LRFD* Articles, the calculation is organized by those three components. Relevant information such as cross-section views, if not included in this document, can be found in the original design example. For reference, a framing plan adapted from Barth (2015) is provided below.

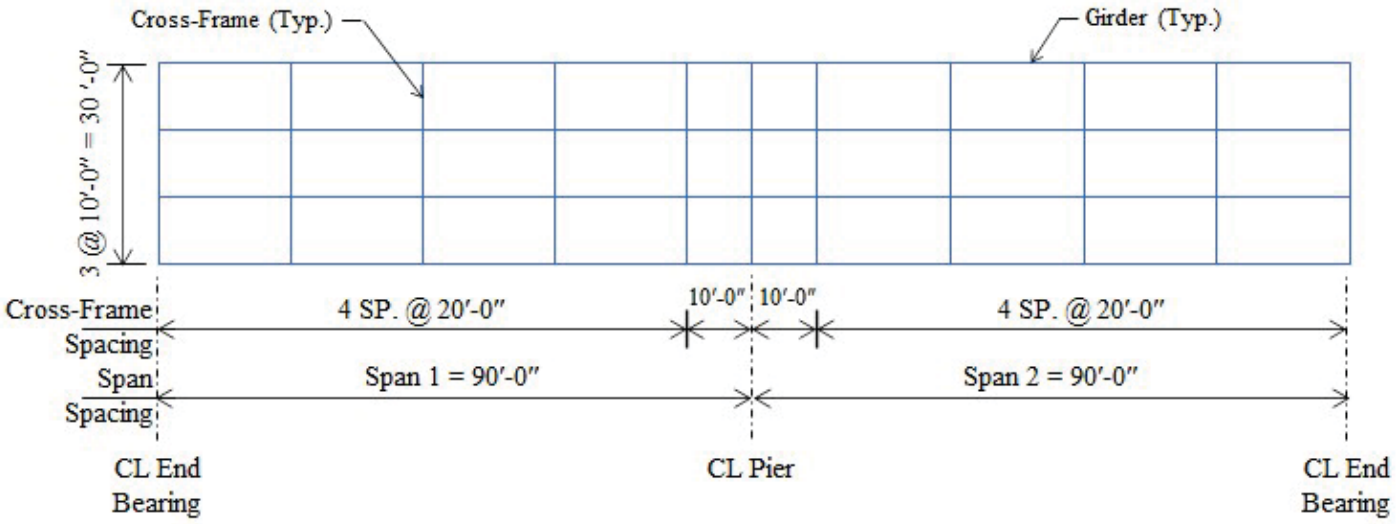

Figure 1: Sketch of superstructure faming plan of bridge; adapted from Barth (2015)

Parameters highlighted in yellow are user inputs (e.g., geometric properties, material properties, design constants). Parameters that are not highlighted have either been previously defined or are functions of other values input by the user. Results highlighted in red are key design loads or resistances, and final design checks are highlighted in orange.

AASHTO LRFD Overview

As outlined in Article 6.7.4, cross-frames shall be investigated for all stages of assumed construction procedures and the final condition. Cross-frames serve many purposes and resist a variety of loads throughout the life of a bridge. Those loading conditions, for which a designer should consider in design, include the following:

- Transfer of lateral wind loads from the bottom of the girder to the deck and from the deck to the bearings;
- Provide lateral support to the fascia girders between cross-frame locations to control torsional stresses and rotations due to loads applied to the overhangs, particularly during concrete deck placement;
- Control stability of the girder in the negative and positive moment region by restraining twist of the cross-section prior to curing of the concrete deck;
- Consideration of any flange lateral bending effects; and
- Distribution of vertical dead and live loads applied to the structure.

Also documented in Article 6.7.4, cross-frames shall be designed for all applicable limit states, if included in

the structural model used to determine force effects. This is particularly true for horizontally-curved bridges that exceed one or more of the conditions specified in Article 4.6.1.2.4 for neglecting the effects of curvature. In these cases, the force effects in cross-frames (considered primary members) shall be computed, and all applicable limit states shall be considered in the design of the member and connections. For straight bridges, at a minimum, cross-frames shall be designed to transfer wind loads according to the provisions of Article 4.6.2.7 and shall meet all applicable slenderness requirements in Article 6.8.4 or Article 6.9.3. Although, as recommended by NCHRP 12-113, stability bracing should also be considered a minimum design requirement.

SBDH Example 2A represents a two-span, continuous bridge with normal supports. Therefore, cross-frames are considered secondary members, which are not often comprehensively designed for all limit states. Instead, cross-frames in these types of bridges are typically sized to only transfer wind loads to the concrete deck in accordance with Article 6.7.4. As such, intermediate cross-frames were designed only to distribute wind loads in the original SBDH Example 2A document. Additionally, the cross-frames are spaced at 20 feet on center typically and are placed in contiguous lines parallel to the normal supports, a layout that is in compliance with the guidelines provided in Article 6.7.4.2.

To better understand the full response of cross-frames during construction and in the final composite structure, this extended design calculation evaluates additional load conditions including: overhang construction, stability bracing during steel erection, dead loads, and vehicular live loads. Wind loads, overhang construction, and stability bracing loads are commonly determined by simple hand calculation methods. The method for determining dead (staged construction and final constructed state) and live load force effects in cross-frames generally depends on the bridge geometry. For a simple framing system like the bridge at hand, dead and live cross-frame forces are typically considered small enough to ignore in design (hence the minimum design requirements outlined above).

In terms of obtaining girder force effects for this type of bridge, simple 1D line-girder or 2D analyses are commonly performed. Note that, for the original SBDH calculation, a line-girder analysis was conducted to determine girder design moments and shears. A more detailed discussion on these load cases in the context of cross-frames is provided in subsequent sections.

Analysis Techniques

As noted previously, dead and live cross-frame force effects in straight and normal bridges have been shown to generally be small in magnitude. As a result, refined analysis methods (either 2D or 3D techniques) are not often conducted for simple framing systems, and design forces for these loading conditions are not explicitly obtained. If a designer elects to obtain cross-frame force effects from a refined analysis for a straight and normal bridge, 2D methods are typically preferred due to their simplicity and ease-of-use.

The results of NCHRP 12-113 confirmed this assertion by establishing geometric limits (i.e., based on the skew and connectivity index) on when live load cross-frame forces are substantial enough to warrant a refined analysis. The bridge at hand, given its straight and normal framing plan, does not satisfy those limits such that no additional analysis is recommended. It is acknowledged that refined models, particularly 3D models, would not typically be used to analyze a simple bridge structure like this. With that in mind, this design example still explores 2D and 3D refined analysis techniques to obtain dead and live load force effects in cross-frames for two different reasons.

The first reason for this approach is to quantitatively confirm that live load forces in critical cross-frame members are small in magnitude, which in turn supports the statements above. Secondly, both 2D and 3D analysis techniques are explored as a means to compare and contrast the performance of each method. In general, it has been observed that 3D models produce more reliable cross-frame results than comparable 2D models given that the depth of the superstructure is explicitly considered and that they do not rely on overly simplistic postprocessing tools.

It is important to note that, despite presenting them herein, this design example is not advocating the use of refined analyses for simple structures, especially 3D methods. Rather, this example serves as an opportunity to demonstrate the proposed modifications to AASHTO LRFD based on the findings of NCHRP 12-113. With that in mind, the remainder of this section is dedicated to outlining the 3D and 2D modeling techniques implemented.

The analysis models developed both qualify as refined analysis techniques, as defined in Articles 4.4 and 4.6.3. A relatively common commercial software package was utilized to build the structural models. The geometry was developed in accordance with the geometric parameters outlined in the original Design Example 2A document (Barth 2015), and the models are representative of what most design engineers would develop for a comparable bridge structure. A staged construction analysis, as well as the final constructed condition, were evaluated. First-order analyses were conducted for all stages of construction.

The 3D model was comprised of shell elements for deck and girder elements and pin-ended truss elements for cross-frame members. Composite action was simulated by vertically offsetting and restraining relative movement between nodes in the top flange and deck shells. Bearings were modeled as linear spring elements, whose lateral stiffness is consistent with common bearings documented in Section 14 of AASHTO *LRFD*.

Another focal point of NCHRP Project 12-113 was the development of appropriate modification factors for eccentrically-loaded single-angle members, from which cross-frames are commonly constructed. Cross-frame systems, which consist of connection plates, gusset plates, and angle members connected via welds and/or bolts, are typically simplified in 3D structural analysis models as pin-ended truss elements. The assumed stiffness, with no modification factor, is generally greater than the true stiffness. It is imperative that the engineer represent the actual stiffness of the cross-frame in the analysis model; overestimating the cross-frame stiffness is conservative from a fatigue perspective but unconservative from a stability bracing perspective.

AASHTO *LRFD* 9th Edition recommends applying a uniform modification factor of 0.65 (C4.6.3.3.4) based on the research conducted by Battistini et al (2016) for stability-related applications. From the work conducted as part of NCHRP 12-113, it is recommended that an R-factor of 0.75 is more appropriate for the response of cross-frame systems in composite structures subjected to traffic loads. This modification factor can either be assigned to the cross-sectional area of the truss element or the modulus of elasticity of the material properties. Note that R = 0.65 is still appropriate for the construction condition.

It was also shown from the results of NCHRP 12-113 that modeling the cross-frame members as eccentric beam elements produces accurate force predictions when compared to a model comprised of shell-element cross-frames. This method is an acceptable alternative to the R-factor approach but is not demonstrated in this example. For reference, a screenshot of the 3D model during its final constructed stage is presented.

In-service modification factor: $R_{ser} := 0.75$

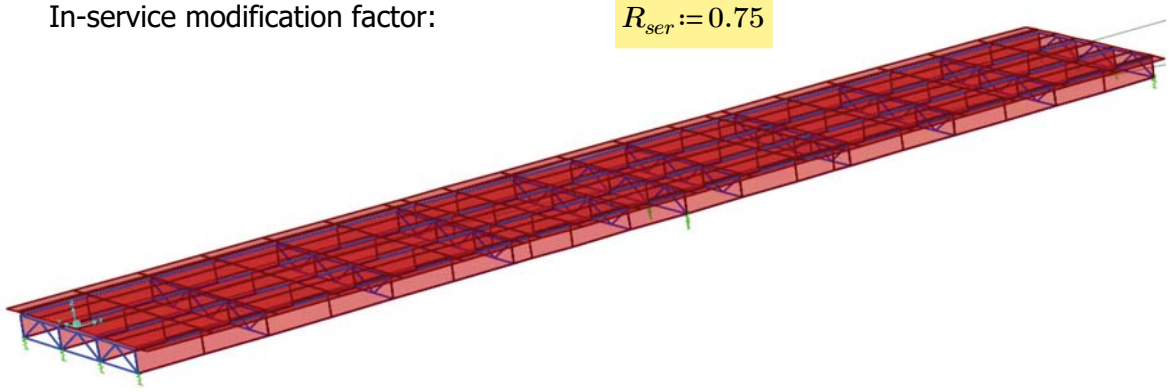

Figure 2: Screenshot of the 3D analysis model

In terms of the comparative 2D analysis, a plate-and-eccentric beam (PEB) model was developed, where cross-frames were represented as equivalent beam elements. The Timoshenko approach was used to determine section properties of the equivalent cross-frame beams in accordance with NCHRP Report 725 (White el al, 2012) and AASHTO G13.1 Guidelines (2014). This approach satisfies the requirements established in current Article 4.6.3.3.4 (or proposed Article 4.6.3.3.4a) that both flexural and shear deformations are considered in determining the equivalent stiffness. Girders, also represented as beam elements, were positioned vertically at the centroid of the cross-section and were constrained to the deck shell to simulate composite action (for the appropriate load cases). The equivalent torsion constant, documented in the AASHTO G13.1 Guidelines, was also applied to girder elements to account for warping stiffness.

To estimate the live-load force effects in the cross-frame members for both strength and fatigue limit states, an influence-surface analysis was conducted. Influence-surface analyses facilitate the handling of moving loads in design; many commercial software packages have built-in capability to perform this special analysis. If not inherently built into the program, the engineer is still tasked with simulating a moving load in various transverse lane positions.

As observed from NCHRP Project 12-113, the induced axial force in a cross-frame member is highly sensitive to load position relative to the cross-frame panel of interest. For bridges with no support skew, the critical loading position is generally localized about the longitudinal position of the cross-frame (i.e., loads applied 50 feet or more away from the cross-frame result in negligible force effects in the cross-frame member of interest). The governing cross-frame panel will typically be near the location of maximum dead load moment (i.e., midspan for single spans and interior span of continuous units; about 0.35L to 0.40L from the end support in exterior spans of continuous units). In contrast, the load influence in skewed and/or curved bridges is more variable, especially for cross-frames near end and intermediate skewed supports. For this reason, an influence-surface analysis, or an equivalent method, is recommended to ensure the critical load position is captured in accordance with Article 3.6.1.4.3.

To satisfy this requirement, an influence-surface grid of 5 feet (longitudinal) by 4 feet (transverse) has been shown to adequately capture the maximum force effects (although a more refined grid could also be implemented). The loading grid was consistent across both modeling approaches, 2D and 3D. The results of this analysis are summarized in the next section.

Force Effects

The following sections outline the development of design force effects for the following load cases: wind on structure, construction, stability bracing, dead, and live loads. For the sake of clarity, only force effects on a single, critical cross-frame member are reported (bottom strut in an end bay near the maximum positive dead load moment region).

Wind on Structure

As discussed in a preceding section, force demands in cross-frame elements due to wind are typically determined using hand solutions but can also be determined with refined analysis. Wind pressure acting normal to the bridge fascia should be considered in design during construction and in the final composite system. The original SBDH Design Example 2A document included a cross-frame design check under construction wind loads only. The calculations herein expand on the original design checks but also evaluate wind demands in the final constructed state. The same general procedures, though, are used.

To determine the wind force demands in the intermediate cross-frames, Article 4.6.2.7 is followed. During construction prior to the composite system, the design wind pressure acting on the fascia girder is distributed longitudinally based on the tributary area associated with the cross-frame spacing. That effective wind force is then equally distributed to the top and bottom struts of the end-bay cross-frame. Wind loads are then distributed to the adjacent girders through the cross-frame truss systems. Ultimately, the critical cross-frame

members in these K-frame panels under this loading condition are the top and bottom struts in the end bay, for which the full effective wind loads act.

In the composite system, wind pressures acting on the upper half of the fascia girder are assumed to be absorbed by the large diaphragm (concrete deck). Wind pressures acting on the lower half of the fascia girder, however, are assumed to pass through the bottom struts, into the diagonals, and into the diaphragm (assuming there is no lateral bracing present). Still, the critical cross-frame member under this loading condition is the bottom strut in the end bay. Both the construction and final conditions are evaluated herein.

In terms of design loads, the original SBDH example designed the cross-frames for 50 psf wind pressures (unfactored), which is reasonable for strength limits states in the final constructed state. Section 3.8 of AASHTO LRFD has changed considerably since the original design example was published. Considering that wind load provisions are not the primary focus of this design example, 50 psf is adopted as the Strength III design pressure in the final bridge without further investigation. To remain consistent with Table 3.8.1.1.2-1, the Strength V wind pressure is taken as 50 psf multiplied by the squared ratio of (80 mph / 115 mph), or 24 psf. The design construction pressures are typically limited to due to wind restrictions during steel erection and deck casting. Construction activity is generally limited to 20 mph wind speeds, which corresponds to approximately a 2-psf wind pressure.

The process for determining the effective wind force acting at the top and bottom struts is similar for construction conditions and the final bridge structure, except that only the bottom struts are considered in the final condition. A sketch is provided, representing wind loading during construction. Relevant design pressure and cross-frame spacing parameters are outlined below. Note that the depth of fascia is conservatively taken as the maximum depth of the nonprismatic, steel girder over its length.

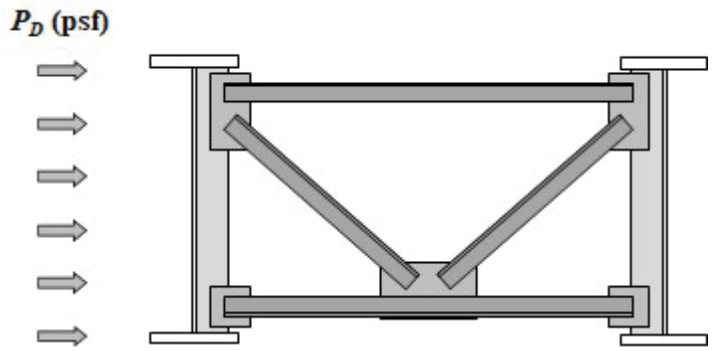

Figure 3: Schematic of wind load applied to the fascia girder

Design pressure, Strength III:	$P_{D.str3} := 50\ psf$
Design pressure, Strength V:	$P_{D.str5} := 24\ psf$
Design pressure, Construction:	$P_{D.c} := 2\ psf$
Unbraced length; critical cross-frame spacing:	$L_b := 20\ ft$
Depth of fascia:	$d := 44.375\ in$

Following Article 4.6.2.7, the process for determining the design force in the critical struts is similar for all construction stages and limit states. The process is summarized with the calculations below. Note that these values represent the compression force (reported as negative value) acting on the governing top or bottom strut in the end bay nearest to the fascia subjected to the windward pressures. These unfactored loads are subsequently factored later in the load combinations and limit states discussion.

Effective strut load, Strength III: $P_{w.str3} := -P_{D.str3} \cdot L_b \cdot \frac{d}{2} = -1.8\ kip$

Effective strut load, Strength V: $P_{w.str5} := -P_{D.str5} \cdot L_b \cdot \frac{d}{2} = -0.9\ kip$

Effective strut load, Construction: $P_{w.c} := -P_{D.c} \cdot L_b \cdot \frac{d}{2} = -0.07\ kip$

Overhang Construction

Similar to wind loads, overhang construction loads are typically computed by simple hand methods. To resist the external torque applied to the fascia girders, cross-frames distribute the vertical and horizontal loads on the girders, as well as provide a support for out-of-plane bending of the flanges (i.e., mitigate lateral flange stress effects). The original SBDH Example 2A document calculated overhang loads to evaluate the lateral bending stresses induced in the fascia girder flanges only. In this extended calculation, those same loads are used to calculate the force demands in the critical cross-frame elements.

In the original design example, the various self-weight and construction loads were identified and quantified. The self-weight components represent the overhanging portion of the wet concrete deck. The construction loads represent the overhang deck forms, the screed rail, a protection railing, a walkway, and the finishing machine. Other than the moving finishing machine, all loads were presented as vertical line loads acting at an offset distance from the vertical plane of the fascia girder. The summation of the vertically applied loads are summarized below. Due to the assumed incline of the overhang bracket, a horizontal force couple is also imparted on the girder flanges, which is the focus herein. A sketch from the original calculation is provided for reference.

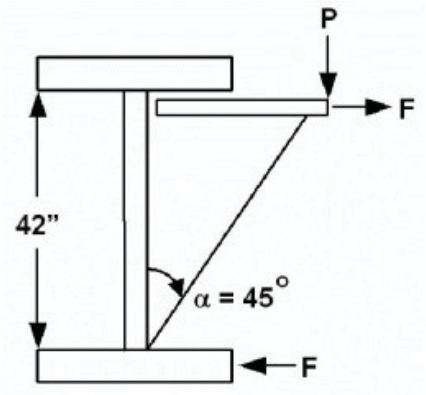

Figure 4: Schematic of construction overhang loads applied to the fascia girder (Barth 2015)

Uniform load, structure weight: $w_{oh.str} := 209\ plf$

Uniform load, construction weight: $w_{oh.c} := 275\ plf$

Concentrated load, construction weight: $P_{oh.c} := 3000\ lbf$

Overhang bracket incline angle: $\theta := 45\ deg$

These vertical and horizontal loads are then assumed to be distributed to each intermediate cross-frame line based on a tributary area. In other words, the line loads are multiplied by the spacing between each intermediate cross-frame along the fascia girder, except for the machine load which can move to any critical load position. The horizontal component of the applied acting on the bottom flange (and resisted by the bottom strut in the end bay) is determined by applying basic principles of statics. The vertical component of the applied load is resisted by the cross-frame diagonal member framing into the top flange and through girder shear. As such, it is not considered in the design and analysis of the critical bottom strut member.

These procedures are demonstrated below. Note that the self-weight and the temporary construction loads are computed separately because each will be assigned a different load factor later in the calculation set. Recall that compression loads are reported as negative values.

Effective strut load, structure weight: $P_{oh.str} := -w_{oh.str} \cdot L_b \cdot \tan(\theta) = -4.2\ \textit{kip}$

Effective strut load, construction weight: $P_{oh.c} := -(w_{oh.c} \cdot L_b + P_{oh.c}) \cdot \tan(\theta) = -8.5\ \textit{kip}$

Stability Bracing - Strength

As introduced above, cross-frames are intended to brace longitudinal girders during construction and in the final constructed state. In order to adequately brace girders from out-of-plane buckling, braces must provide adequate strength and stiffness. Braces can either be categorized as lateral braces (preventing out-of-plane lateral movement of the compression flange) or torsional braces (preventing relative twist of the cross-section about its shear center). The most common form of bracing in steel I-girder bridges are cross-frames, since they control girder twist at discrete locations along the length (i.e., torsional braces).

Currently, AASHTO *LRFD* 9th Edition provides no guidance on how to properly design and detail cross-frames to serve as braces. As part of NCHRP Project 12-113, many of the provisions documented in Appendix 6.3 of the AISC Specifications (2016) were evaluated for their implementation into AASHTO. In particular, the torsional brace stiffness and strength requirements were studied for common bridge systems. The calculations herein demonstrate the proposed modifications to these AISC provisions.

First, the required strength of the torsional brace is calculated. In other words, the force imparted on the cross-frame as the girder approaches its critical buckling moment is computed. Note that a separate check will be provided later to investigate the required stiffness of the cross-frame to serve as a brace. The required strength of a point, torsional brace is computed by the following equation:

$$M_{br} := \frac{0.036\ M_r \cdot \boldsymbol{L}}{n \cdot C_b \cdot L_b}$$

This equation is based on the findings Liu and Helwig (2020a). Current 15th Edition AISC Specifications (2016) require a brace moment equivalent to 2% of the factored flexural moment in the girder span, which is independent of the bracing scheme of the girder. Liu and Helwig (2020a) showed that brace moment typically exceeds 2% of the girder moment. Thus, for implementation into AASHTO *LRFD*, it was proposed to adopt the equation above, which is a similar form to the equation presented in the 14th Edition of AISC (2010).

The required brace strength is based on an assumed critical imperfection of $L_b/500$, where the compression flange has a lateral sweep at the critical brace location and the tension flange remains straight (Han and Helwig, 2020). The original 14th Edition AISC equation is derived from the assumption that twice the ideal torsional stiffness is required to limit the out-of-plane deformations incurred at the critical buckling load. Liu et al. (2020b) demonstrated that three times the ideal stiffness is more appropriate for beam buckling applications. As such, the equation above modifies the AISC (2010) equation to consider a cross-frame stiffness equivalent to three times the ideal stiffness. Hence, the constant is increased 50% from 0.024 to 0.036.

As noted in the NCHRP 12-113 final report, bracing strength requirements are critical for the noncomposite condition of the bridge (i.e., during construction). In the composite system, lateral-torsional buckling of the longitudinal girders is generally not critical at the intermediate support due to the restraint provided by the bearings and concrete deck. The bearings and deck provide restraint to twisting of the cross-section even in systems where shear studs are omitted in the negative moment region. In the negative moment regions of continuous systems, web distortional buckling, which is not significantly affected by the unbraced length, is much more critical than conventional LTB, particularly for slender unstiffened webs (Helwig and Yura, 2015). Web distortional effects, although important to girder design, are not evaluated in this calculation set.

With these factors in mind, the bracing requirements are evaluated at all critical stages of construction. In this example, the critical stage for stability bracing is during deck construction before the concrete has cured.

The deck forms provide no buckling restraint to the girders as the connections are often flexible, such that the cross-frames are the sole source of stability bracing (assuming no temporary, external bracing mechanisms are provided by the erector). Although only one stage of construction is explicitly considered in this example, it is important to examine all potentially critical stages, particularly those where permanent bracing is not fully installed and girders may be subjected to long unbraced lengths. For all construction stages examined, it is imperative that the the appropriate M_r term in the bracing strength equation is considered. Additionally, only load cases that act concurrently with the critical construction stage should be considered in the load combination. For instance, overhang deck construction loads need not be combined with stability bracing forces corresponding to intermediate phases of steel erection, as these conditions are not concurrent.

As such, the focus of this design example is related to stability bracing demands directly after the deck is cast and the concrete is still wet. To satisfy the bracing strength requirements, both the critical positive and negative moment regions must be evaluated for this continuous span. This is achieved by designing all cross-frame braces in the span for the maximum value of M_r/C_bL_b. For this example, two different unbraced segments are checked: the one containing the maximum positive moment and the one containing the maximum negative moment (i.e., the end segment).

Before presenting those calculations, it should be noted that the L_b value to consider need not be taken less than the maximum unbraced length permitted for the beam to reach the required flexural strength, M_r. This provision accounts for scenarios in which the spacing of the brace is significantly less than is required to develop the strength of the beam. In essence, this provision lessens the demands on cross-frames for girders that would not buckle under the specified cross-frame layout (i.e., the girder would partially or fully yield prior to buckling). In this particular example, the end segment has an unbraced length of 10 feet, which is nearly equivalent to L_p, the limiting unbraced length to achieve the nominal resistance of the girder cross-section under uniform bending. Thus, it is evident that increasing the L_b value in the denominator of the equation above is warranted, as this segment (although subjected to the largest moment magnitude) is controlled by yielding and not LTB. Lastly, because the individual spans of this bridge are identical in terms of length, L, and number of intermediate braces, n, only one calculation is needed.

The moment diagram below is taken from the original design example and serves as the basis for the bracing strength requirements. Note that these results were obtained from a line-girder analysis and AASHTO load distribution factors. The 3D and 2D analysis models, performed as part of these calculations, reported similar girder force effects but are not explicitly shown herein.

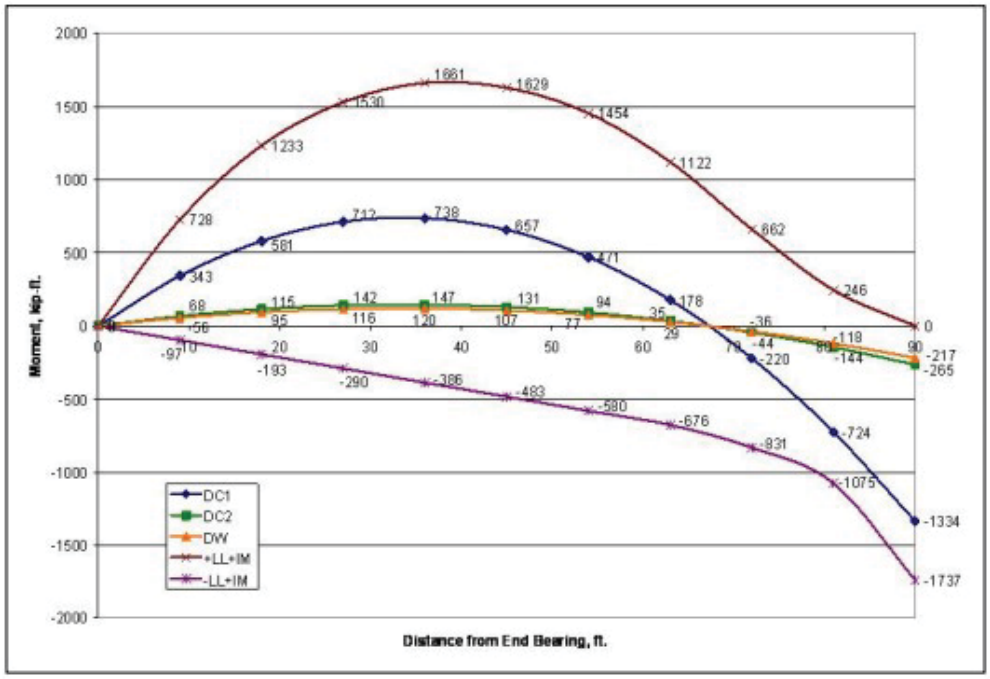

Figure 5: Unfactored moment diagram of the critical span (Barth, 2015)

First, the critical unbraced segment in the positive moment region is checked. In this particular instance, the girder moment is taken as the maximum positive moment caused by DC1 loads (i.e., the dead loads acting concurrently with the critical stage of construction considered). Note, however, that M_r term in the equation is based on the factored girder moment. Because two different limit states and load combinations were evaluated that consider stability bracing requirements, these bracing forces are subsequently factored later in the calculation set. Thus, the required brace moment is presented as an unfactored magnitude for now.

Span length: $L := 90\ ft$

Number of intermediate braces: $n_b := 4$

Maximum girder moment in segment: $M_r := 738\ kip \cdot ft$

The L_b term to consider, as noted above, need not be taken less than the maximum unbraced length permitted for the beam to develop its required flexural strength, M_r. As such, Article 6.10.8.2.3 was utilized to determine the maximum unbraced length that the positive-moment girder segment could have, for which its LTB capacity still exceeds the required strength (taken as 1.4 times M_r, or 1033 k-ft, to represent the critical construction load combination outlined below). Considering the steel section properties only (i.e., no composite properties for this stage of construction) and taking C_b as 1.0, it was determined that the maximum L_b value is almost 35 feet. These calculations are presented below for reference.

Many of the notable parameters, including the effective radius of gyration for LTB and the web load-shedding factor, are taken directly from the original design calculation. Eq. 6.10.8.2.3-3 in AASHTO LRFD, the elastic LTB expression which conservatively neglects the torsion constant term, is rearranged in such a way that the L_b required to equate the required strength and applicable LTB capacity can be computed. Note that the moment gradient factor was conservatively taken as unity to simplify the calculation. As L_b increases, C_b slightly changes but is generally not much larger than 1.0.

Moment gradient factor: $C_b := 1.0$

Web load-shedding factor: $R_b := 1.0$

Effective radius of gyration for LTB: $r_t := 3.48\ in$

Section modulus, top compression flange: $S_{xc} := 614\ in^3$

Modulus of elasticity, steel: $E := 29000\ ksi$

Maximum permissible unbraced length to develop maximum positive girder moment (1033 kip-ft):

$$L_b := \sqrt{\frac{C_b \cdot R_b \cdot \pi^2 \cdot E \cdot r_t^{\,2} \cdot S_{xc}}{1.4\ M_r}} = 34.5\ ft$$

Lastly, the C_b term used in the bracing strength equation, despite the discussion above for computing the appropriate unbraced length, is based the moment gradient factor in the actual unbraced segment. Calculations show, however, that C_b is nearly unity for the specified 20-foot unbraced segment and the moment diagram above. Therefore, it conservatively taken as 1.0.

Moment gradient factor: $C_b := 1.0$

With each parameter established, the required torsional brace strength for the positive-moment segment is given by the following:

$$M_{br.pos} := \frac{0.036\ M_r \cdot L}{n_b \cdot C_b \cdot L_b} = 17.3\ kip \cdot ft$$

Now, the critical unbraced segment in the negative moment region is checked. In this case, the maximum girder moment is taken as the maximum negative moment caused by DC1 loads (i.e., the dead loads acting

concurrently with the critical stage of construction considered).

Maximum moment in girder moment (unfactored): $M_r := 1334\ \textit{kip} \cdot \textit{ft}$

Similar to the procedure outlined above, Article 6.10.8.2.3 was utilized to determine the maximum unbraced length for the critical negative-moment girder segment. The notable differences between the positive and negative moment calculations are the girder section properties used (i.e., the web and flange dimensions are larger in the negative moment region) and the moment gradient factor. To simplify the calculations, C_b was conservatively taken as 2.0. Again, C_b slightly changes as L_b increases, but a conservative estimate of the moment gradient factor for reverse-curvature bending is 2.0. With those factors in mind, it was determined that the maximum L_b value is nearly 50 feet which is substantially larger than the actual unbraced length of 10 feet. These calculations, which are similar to those presented above for the positive moment region, are not presented herein.

Maximum permissible unbraced length to develop maximum negative girder moment (1.4 x 1334 kip-ft): $L_b := 50\ \textit{ft}$

Despite the discussion above, the C_b factor corresponding to the actual 10-foot unbraced segment and moment diagram is approximately 1.27 using AISC Specifications guidance (Equation F1-1).

Moment gradient factor: $C_b := 1.27$

Thus, the required torsional brace strength for the negative moment region segment is given by the following:

$$M_{br.neg} := \frac{0.036\ M_r \cdot L}{n_b \cdot C_b \cdot L_b} = 17.0\ \textit{kip} \cdot \textit{ft}$$

For simplicity, the same cross-frame size is used throughout. Therefore, the appropriate brace moment, for which all cross-frames in the span would be designed, is the largest of the two segments presented above.

$$M_{br} := \max\left(M_{br.pos}, M_{br.neg}\right) = 17.3\ \textit{kip} \cdot \textit{ft}$$

The torsional brace moment is then converted into a force couple acting at the top and bottom of the cross-frame trusswork. Provided that a girder can buckle out of plane in either direction depending on the nature of its imperfections, the sign of the force couple can vary. In terms of the bottom strut design throughout this calculation set, a compression load is more critical. Therefore, the unfactored force demand due to stability bracing is taken as the value below in terms of compression (reported as negative value). This force effect will be appropriately factored and combined with wind and construction loads at the end of the calculation set. This procedure is demonstrated schematically in the figure below.

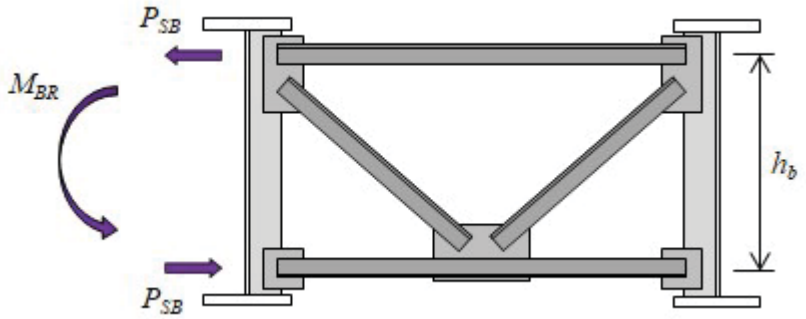

Figure 6: Schematic demonstrating the development of stability bracing forces in cross-frames

Height of cross-frame brace: $h_b := 30\ \textit{in}$

$$P_{sb} := -\frac{M_{br}}{h_b} = -6.9 \ kip$$

Dead Load

As documented extensively in Article 6.7.2 and its associated commentary, there are two different types of dead load forces that act on a cross-frame throughout its life: the internal dead load forces and the "fit-up" forces, which are external forces that the erector may need to apply to assemble the structural steel during erection. The fit-up forces are largely dependent on which fit condition is selected by the engineer and built by the steel erector. The three most common fit conditions are: (i) no-load fit (NLF), (ii) steel dead load fit (SDLF), and (iii) total dead load fit (TDLF). The original SBDH example problem did not specify the intended fit condition. Given that the bridge is straight with normal supports, the calculations herein assume the NLF condition. This assumption is acceptable per NCHRP 20-07/Task 355 Report, the governing research document that investigated the fit conditions of cross-frames.

NLF implies that the cross-frames are installed in a "zero load condition" when the girders are plumb (i.e., steel framing erected on the ground). Therefore, the external forces required to fit the cross-frames are assumed negligible. With that in mind, only the internal dead load forces developed during construction need to be considered in the design of the cross-frames in this example. For different fit conditions particularly in skewed and/or curved bridges, refer to Article 6.7.2 or NCHRP 20-07/Task 355 (White et al. 2015) for refined analysis techniques and simplified methods for estimating these locked-in force effects.

Girders in straight bridges with normal supports typically deflect uniformly, and twist of the cross-section is negligible. Thus, the internal dead load forces due to construction and self-weight material loads are typically small for these types of bridge superstructures and are often neglected in design. Still, 2D and 3D refined analysis models were developed to capture the effects of staged construction to verify this assertion.

Internal dead load force effects in cross-frames under the NLF assumption are essentially determined by applying and combining gravity loads at every stage of construction: steel erection, installing formwork, deck casting (staged or simultaneous pour), barrier casting, and wearing surface pour. To remain consistent with the original design example, two different deck pour scenarios were considered: (i) a two-pour scheme as demonstrated by Figure 15 in the original SBDH example and (ii) a single continuous pour scheme. Ultimately, the design loads are governed by the more critical scenario.

The steps below outline the dead load forces due to all intermediate stages of construction. They are organized and designated as DC1 (dead loads applied to the noncomposite system), DC2 (dead loads applied to the composite system), and DW (wearing surface loads applied to the composite system). To remain consistent with the wind and overhang loads described above, only the most critical bottom strut member in the end bay is evaluated. As expected, the critical bottom strut member was found to occur at in the maximum dead load moment region where girder deflections are greatest (i.e. approximately 0.35L measured from the end support). Note that, although not explicitly presented here, similar calculations shall be made for other cross-frame members that may control the design.

In terms of DC1 loads, the self-weight of the steel framing, the stay-in-place deck forms, and the concrete deck (including haunch and overhangs) were considered. These loads are assumed to act on the noncomposite system (or steel section alone). Deck forms were assumed to weigh 15 psf in accordance with the original design example. From a staged construction analysis, the following DC1 force effects were provided by the 3D analysis model for the critical bottom strut member:

Dead load, steel framing:	$P_{dc.s} := 0.00 \ kip$	(0.00 kip)
Dead load, formwork:	$P_{dc.f} := 0.62 \ kip$	(0.59 kip)
Dead load, wet concrete deck:	$P_{dc.d} := 0.10 \ kip$	(0.31 kip)

Note that the results from the 2D PEB analysis and postprocessing are provided in parentheses for reference. Using the 3D analysis results, the combined DC1 force effect in the critical bottom strut member is as follows (all loads in tension):

$$P_{dc1} := P_{dc.s} + P_{dc.f} + P_{dc.d} = 0.72\ kip$$

DC2 loads, in this case, are comprised solely of barrier loads since the bridge is assumed to have no sidewalks and medians. The barrier weight is taken as 520 plf to replicate the original design example. When performing hand calculations, barrier loads are often distributed equally to all girders across the width. In the refined analysis model, each barrier load is applied at a 1-foot offset distance from the deck edge, and the model distributes the load based on stiffness in accordance with Article C4.6.1.2.4b. The load is applied to the long-term composite structure. The following DC2 force effect was determined for the critical bottom strut member (2D results in parentheses):

$$P_{dc2} := -3.65\ kip \qquad \text{(-4.54 kip)}$$

Future wearing surface loads, like DC2 loads, are assumed to act on the long-term composite system and are typically distributed equally to all girders in hand calculations. Applying a 25 psf load to the deck and running the analysis model, the following DW force effect was determined for the critical bottom strut member (2D results in parentheses):

$$P_{dw} := -0.78\ kip \qquad \text{(0.37 kip)}$$

It is evident from the magnitudes of these loads that dead load effects on cross-frames in straight and normal systems are relatively small. The 2D analysis model produced cross-frame forces in good agreement with the 3D analysis as well, particularly for the load cases performed on the noncomposite system (i.e., DC1 loads). This noted behavior is consistent with the findings of NCHRP 12-113. Although accurate for noncomposite systems, 2D analyses tend to produce more substantial errors with live load cross-frame forces, which is largely attributed to the inherent postprocessing assumptions.

According to both 3D and 2D analyses, the barrier DC2 load produces the the highest force effects due to the eccentric nature of loading on the bridge deck (i.e., slight differential deflection and twist of the fascia girders relative to the interior girders). The force effects outlined above are appropriately factored and combined with wind, construction, stability bracing, and live loads later in the calculation set.

Live Load and Impact

Similar to dead loads, live load force effects were determined from the 3D and 2D analysis models. The influence-surface procedure outlined previously was performed. The result of the influence-surface analysis is a color contour plot, which demonstrates the axial-force response of the select bottom strut cross-frame member due to a 1-kip load positioned at a given spatial coordinate on the deck surface. For the member of interest, the corresponding contour plot is presented below for reference.

For loads applied in the "red" area on the plot, the compression force in the bottom strut is maximized. For loads in the "blue" area, the tension force in the bottom strut is maximized. Load positions in grey have negligible influence on the axial-force response in that cross-frame. In terms of design loads, strength and fatigue limit states are handled differently. For the strength limit state, loads in accordance with Article 3.6.1.3 were applied. For the fatigue limit state, loads in accordance with Article 3.6.1.4 were applied. The commercial software package was utilized to apply these separate loading conditions, and the results were validated with hand solutions. To demonstrate one example, the influence-line response of the bottom strut member due to the AASHTO fatigue truck is presented below. In this example, the fatigue truck traverses the length of the bridge (left to right orientation in influence surface) with its right wheel riding nearly over the third girder (located at transverse position of +8.5 on influence surface). This process was repeated for all transverse lane positions in both the forward and backward directions to ultimately find the governing

force demands.

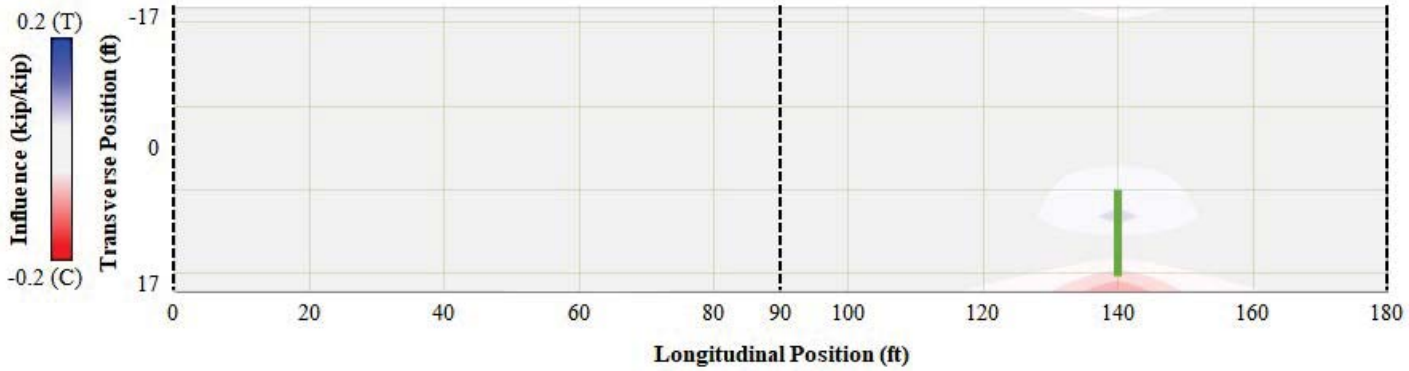

Figure 6: Influence-surface plot generated for the critical cross-frame member

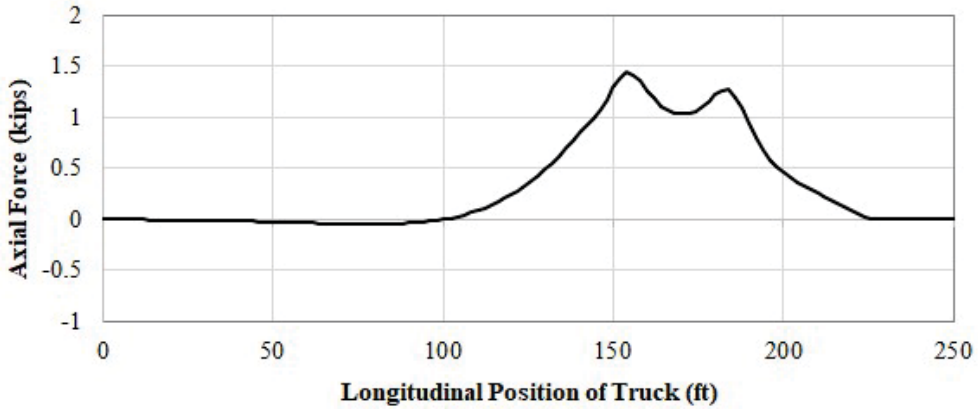

Figure 7: Sample influence-line plot generated for the critical cross-frame member

The force effects below summarize the output from the 3D analysis model (and 2D model in parentheses) implementing Article 3.6.1.3 (strength) and Article 3.6.1.4 (fatigue) loading criteria. Note that for the strength limit state, the maximum tension and compression forces are recorded; for the fatigue limit state, the critical total force range is recorded. The critical force range for fatigue was determined based on Article C6.6.1.2.1 (i.e., any stress/force cycle that has a tensile component). Note that the appropriate impact factors are also included in the reported results. A dynamic load allowance factor of 0.33 is applied to the design truck or tandem in the strength limit state, and a factor of 0.15 is applied to the truck in the fatigue limit state. The force effects below are appropriately factored and combined with wind, construction, stability bracing, and dead loads later in the calculation set.

Live load, strength envelope:	$P_{ll.str.t} := 3.58\ kip$	(7.20 kip)
	$P_{ll.str.c} := -2.93\ kip$	(-7.50 kip)
Live load, fatigue force range:	$P_{ll.fat} := 1.64\ kip$	(3.90 kip)

Note that the 2D results overestimated the governing force effects, which is attributed to the postprocessing procedure inherent with this type of analysis. Because 3D results are more reliable, they are used in the design calculations herein.

Limit States and Load Combinations

Now that the unfactored design loads have been established for the critical bottom strut cross-frame member, a discussion on the applicable limit states is warranted. Tables are provided below that identify the appropriate load combinations and load factors to consider. Each of these items is discussed below in the context of cross-frame design.

Following Articles 3.4.1 and 3.4.2, the adequacy of the cross-frames must be evaluated during all construction stages and in the final constructed state using the load combinations in Table 3.4.1-1. Strength I, Strength III, Strength V, Fatigue I, and Fatigue II are specifically addressed. Aside from the main load combinations, there are three additional items to note. First, Article 3.4.2 introduces special combinations for construction loads, which are considered herein. Second, despite not being explicitly considered in Table 3.4.1-1, stability bracing force effects shall also be considered based on the proposed specification language in proposed Article 6.7.4.2.2. Note that the stability bracing load factors are marked with an asterisk in the table below because these force effects are not independently factored. Instead, they are based on the corresponding factored girder moment. Third, the cross-frame-specific load factors proposed as part of NCHRP 12-113 are also included. These values are signified with a double asterisk in the table.

Recall that the following load cases have been evaluated above: dead load (DC1, DC2, DW), live load (strength LL, fatigue LL), overhang construction (CL), wind on structure (construction WS, final WS), and stability bracing (SB). During construction, the critical stage consists of the noncomposite system immediately after deck casting (i.e., wet concrete load). For this condition, two limit states and load combinations have been identified as critical: Strength III and the special construction case. These load combinations are tabulated below:

	DC1	DC2	DW	LL+IM	$(LL+IM)_f$	WS	CL	SB
Strength III	1.25	--	--	--	--	1.25	1.5	*
Construction	1.4	--	--	--	--	--	1.4	*

In the finished bridge when DC2, DW, and LL cases are introduced, additional limit states and combinations are investigated, which are tabulated below.

	DC1	DC2	DW	LL+IM	$(LL+IM)_f$	WS	CL	SB
Strength I	1.25	1.25	1.5	1.75	--	--	--	--
Strength III	1.25	1.25	1.5	--	--	1	--	--
Strength V	1.25	1.25	1.5	1.35	--	1	--	--
Fatigue I	--	--	--	--	1.14**	--	--	--
Fatigue II	--	--	--	--	0.52**	--	--	--

With the limit states established, the next step is to determine the factored combined force effects for the cross-frame member of interest. Note that the ductility factor (Article 1.3.3), the redundancy factor (1.3.4), and the operational importance factor (1.3.5) are all taken as 1.0 in this example. First, the construction-related loads are summarized:

DC1, vertical loads: $P_{dc1} = 0.72$ ***kip***

DC1, overhang loads: $P_{oh.str} = -4.18$ ***kip***

WS, construction: $P_{w.c} = -0.07$ ***kip***

CL, overhang loads: $P_{oh.c} = -8.5$ ***kip***

SB: $P_{sb} = -6.93$ ***kip***

Strength III limit state, construction:

$$P_{c.str3} := 1.25 \cdot \left(P_{dc1} + P_{oh.str}\right) + 1.25 \cdot P_{w.c} + 1.5 \cdot P_{oh.c} + 1.25 \cdot P_{sb} = -25.8 \text{ kip}$$

Construction condition:

$$P_{c.cl} := 1.4 \cdot \left(P_{dc1} + P_{oh.str}\right) + 1.4 \cdot P_{oh.c} + 1.4 \cdot P_{sb} = -26.4 \text{ kip}$$

Note that the stability bracing force effects are shown as being factored because, as previously noted, P_{SB} was initially based on an unfactored girder moment. It is important to avoid "double counting" the load factors in these cases.

Next, the load combinations corresponding to the finished bridge are summarized. Ultimately, compression forces will govern over tension forces for cross-frame single-angle design (except for the fatigue limit state); thus, only the maximum live load induced compression force is presented.

DC1: $P_{dc1} = 0.72\ kip$

DC2: $P_{dc2} = -3.65\ kip$

DW: $P_{dw} = -0.78\ kip$

LL+IM (Strength): $P_{ll.str.c} = -2.93\ kip$

LL+IM (Fatigue): $P_{ll.fat} = 1.64\ kip$

WS, finished (Strength III): $P_{w.str3} = -1.85\ kip$

WS, finished (Strength III): $P_{w.str5} = -0.89\ kip$

Strength I limit state:

$$P_{str1} := 1.25 \cdot \left(P_{dc1} + P_{dc2}\right) + 1.5 \cdot P_{dw} + 1.75 \cdot P_{ll.str.c} = -10\ kip$$

Strength III limit state:

$$P_{str3} := 1.25 \cdot \left(P_{dc1} + P_{dc2}\right) + 1.5 \cdot P_{dw} + 1.0 \cdot P_{w.str3} = -6.7\ kip$$

Strength V limit state:

$$P_{str5} := 1.25 \cdot \left(P_{dc1} + P_{dc2}\right) + 1.5 \cdot P_{dw} + 1.35 \cdot P_{ll.str.c} + 1.0 \cdot P_{w.str5} = -9.7\ kip$$

Fatigue I (infinite life) limit state:

$$P_{f1} := 1.75 \cdot 0.65 \cdot P_{ll.fat} = 1.9\ kip$$

Fatigue II (finite life) limit state:

$$P_{f2} := 0.8 \cdot 0.65 \cdot P_{ll.fat} = 0.9\ kip$$

Therefore, the governing force demands for the strength and fatigue limit states are summarized below (compression forces taken as negative values). Note that the construction stage governs the strength design of the cross-frame of interest. The appropriate fatigue limit state (Fatigue I or II) is determined in the subsequent section.

Strength limit state:

$$P_{str} := -\max\left(\left|P_{c.str3}\right|, \left|P_{c.cl}\right|, \left|P_{str1}\right|, \left|P_{str3}\right|, \left|P_{str5}\right|\right) = -26.4\ kip$$

Fatigue I (infinite life) limit state:

$$P_{f1} = 1.9\ kip$$

Fatigue II (finite life) limit state:

$$P_{f2} = 0.9\ kip$$

Resistance

The following section outlines the development of factored resistances for the critical single-angle bottom

strut member. Strength and fatigue limit states are addressed separately.

Strength Limit State

The original SBDH example problem provided a detailed calculation of the compressive resistance of the bottom strut cross-frame member, which is still applicable to the design example. For completeness, the same calculations are provided with one notable correction. In the original calculation, the angle section was identified as a nonslender section due to an error in reporting the leg thickness; the angle is slender, and the calculations are updated to reflect that. Therefore, the following calculations compute the factored resistance of a L4x4x5/16 single-angle member eccentrically loaded in compression with a 1/2-inch thick connection plate, as well as perform appropriate slenderness checks. The following parameters characterize the cross-section properties of the angle based on Table 1-7 in the AISC Manual (2017).

Gross area of angle: $A_g := 2.40\ in^2$

Radius of gyration, z-axis: $r_z := 0.781\ in$

Radius of gyration, x-axis: $r_x := 1.24\ in$

Radius of gyration, y-axis: $r_y := 1.24\ in$

Leg width: $b := 4.0\ in$

Leg thickness: $t := 0.3125\ in$

Steel material properties are summarized below. Note that grade 50 steel is assumed for the cross-frame elements.

Modulus of elasticity, steel: $E = 29000\ ksi$

Yield strength: $F_y := 50\ ksi$

Next, the slenderness of the outstanding legs (Article 6.9.4.2.1) and the global member slenderness (6.9.3) must be checked. The plate buckling coefficient is taken as 0.45 per Table 6.9.4.2.1-1.

Slenderness of cross-section: $\frac{b}{t} = 12.8$

Plate buckling coefficient: $k := 0.45$

Slenderness limit: $\lambda_r := k \cdot \sqrt{\frac{E}{F_y}} = 10.8$

$$Check := \left\| \begin{array}{l} \text{if } \frac{b}{t} > \lambda_r \\ \quad \| \text{“Slender section”} \\ \text{else} \\ \quad \| \text{“Nonslender section”} \end{array} \right\| = \text{“Slender section”}$$

Since the section is deemed slender, Article 6.9.4.2.2 must be checked. Because the critical global buckling stress needs to be computed in order to calculate the slenderness effects of 6.9.4.2.2, this check is made later. In the meanwhile, the slenderness provision of Article 6.9.3 must also be evaluated. Since the member is considered a secondary member, the slenderness limit is set as 140. Given the length of the connection and gusset plates, the unbraced length of the single-angle bottom strut is taken as 9 feet to maintain consistency with the original design example. The diagonal members framing into mid-length of the bottom strut are not considered effective braces, particularly out of plane. The effective length factor is taken as 1.0 for single members per Article 4.6.2.5.

Effective length factor: $K := 1.0$

Unbraced length: $l := 9\ ft$

Minimum radius of gyration: $r_{min} := r_z = 0.781\ in$

Slenderness of member: $\frac{K \cdot l}{r_{min}} = 138.3$

$$Check := \left\| \begin{array}{l} \text{if } \frac{K \cdot l}{r_{min}} > 140 \\ \quad \text{"Slender; revisit design"} \\ \text{else} \\ \quad \text{"OK"} \end{array} \right\| = \text{"OK"}$$

Having satisfied the basic slenderness provisions, the angle must now be checked for the strength limit state in accordance with Article 6.9.4.4. The cross-frame member of interest, like many single angle sections, is eccentrically loaded due to the connection to the gusset plate through one leg only. Therefore, the member is subjected to axial and flexural stresses, which complicates the calculation of compression resistance. Article 6.9.4.4 employs a simplified approach to computing the resistance. The bending moments are effectively neglected in lieu of assigning an effective slenderness ratio for flexural buckling. Also, per Article 6.9.4.4, single angles designed using this simplified procedure need not be checked for flexural-torsional buckling. The calculation of the effective slenderness ratio is presented herein (for equal-leg angles).

Effective slenderness: $$\lambda_{eff} := \left\| \begin{array}{l} \text{if } \frac{l}{r_x} \le 80 \\ \quad 72 + 0.75 \cdot \frac{l}{r_x} \\ \text{else} \\ \quad 32 + 1.25 \cdot \frac{l}{r_x} \end{array} \right\| = 140.9$$

With the effective slenderness ratio known, Article 6.4.1.1 can be enforced to compute the compression resistance of the member. The nominal resistance is calculated as follows:

Elastic critical buckling resistance: $P_e := \frac{\pi^2 E}{(\lambda_{eff})^2} \cdot A_g = 34.6\ kip$

Nominal yield resistance: $P_o := F_y \cdot A_g = 120\ kip$

Nominal compression resistance: $$P_n := \left\| \begin{array}{l} \text{if } \frac{P_e}{P_o} \ge 0.44 \\ \quad \left(0.6558^{\left(\frac{P_o}{P_e}\right)}\right) \cdot P_o \\ \text{else} \\ \quad 0.877 \cdot P_e \end{array} \right\| = 30.4\ kip$$

Before assigning the appropriate resistance factor, the effective leg width calculation needs to be checked to

ensure local buckling effects will not limit the global buckling capacity determined above. Following Article 6.9.4.2.2a, the effective leg width is determined as follows:

Limiting section slenderness: $\lambda_r := 10.8$

Nominal compression resistance (stress): $F_{cr} := \frac{P_n}{A_g} = 12.6\ ksi$

Limiting slenderness to activate effective leg width: $\lambda_s := \lambda_r \cdot \sqrt{\frac{F_y}{F_{cr}}} = 21.5$

$$Check := \left\| \begin{array}{l} \text{if } \frac{b}{t} \le \lambda_s \\ \quad \| \text{“Use full width”} \\ \text{else} \\ \quad \| \text{“Use effective width”} \end{array} \right\| = \text{“Use full width”}$$

Therefore, local buckling is not a concern as the compressive stress at buckling is too low, and the nominal resistance computed above still applies. Now, the factored resistance is computed per Article 6.5.4.2 and 6.9.2.1.

Resistance factor: $\phi_c := 0.95$

Factored compression resistance: $P_{r.str} := \phi_c \cdot P_n = 28.8\ kip$

The factored compressive resistance is to be compared against the factored force demand determined in the previous section. This check is provided in a subsequent section. Had tensile forces governed the design, refer to Article 6.8 for the appropriate design procedures.

Fatigue Limit State

As suggested in Article 6.6.1.1, both load-induced (6.6.1.2) and distortion-induced (6.6.1.3) fatigue shall be considered in design of cross-frames. For this example, though, it is assumed that the cross-frame and its connection plates are detailed properly in accordance with Article 6.6.1.3 such that distortion-induced fatigue is not a design concern. Therefore, only load-induced fatigue is a design consideration herein. The first step in computing the load-induced fatigue resistance of the single-angle cross-frame member is to establish the fatigue category and its pertinent design parameters. Per Table 6.6.1.2.3-1 (Section 7.2), a single-angle member welded along one side to a connection plate is given the E' designation (McDonald and Frank, 2009). Therefore, the following parameters are used herein:

Detail category constant: $A := 3.9 \cdot 10^8\ ksi^3$

Threshold stress: $\Delta F_{th} := 2.6\ ksi$

Next, the appropriate limit state (Fatigue I versus Fatigue II) must be established. Per Article 6.6.1.2.3, if the projected single-lane Average Daily Truck Traffic (ADTT) is less than or equal to the applicable value in Table 6.6.1.2.3-2, then the member shall be designed for finite-life (Fatigue II). To make that determination, the projected truck traffic on the bridge must be estimated. To maintain consistency with the original SBDH example, a single-lane ADTT of 800 trucks per day is assumed. Therefore, the cross-frame detail shall be designed for the Fatigue II limit state, as demonstrated mathematically below.

Single-lane ADTT: $ADTT_{sl} := 800$

75-year single-lane ADTT equivalent to infinite life: $ADTT_{sl.inf} := 8485$

$$Check := \left\| \begin{array}{l} \text{if } ADTT_{sl} \le ADTT_{sl.inf} \\ \quad \| \text{“Design for Fatigue II”} \\ \text{else} \\ \quad \| \text{“Design for Fatigue I”} \end{array} \right\| = \text{“Design for Fatigue II”}$$

Thus, the nominal fatigue resistance is calculated in accordance with Article 6.6.1.2.5 and Eq. 6.6.1.2.5-2 specifically. To do so, the total number of stress cycles expected on the cross-frame member of interest during the 75-year design span must be computed. This requires an assumption on the number of stress range cycles per truck passage (Table 6.6.1.2.5-2). Based on the findings of NCHRP 12-113, assuming one stress cycle per truck passage for cross-frame members is most appropriate. These calculations are presented below.

Cycles per truck passage: $n := 1.0$

Total design cycles: $N := 365 \cdot 75 \cdot n \cdot ADTT_{sl} = 2.19 \cdot 10^{7}$

Nominal fatigue resistance: $\Delta F_n := \left(\frac{A}{N}\right)^{\frac{1}{3}} = 2.61 \ ksi$

In accordance with Article C6.6.1.2.2, both the resistance factor and the additional load modifiers are taken as 1.0. Therefore, the factored fatigue resistance is taken as the following. Note that fatigue resistance is typically computed in terms of axial stress (i.e., P/A); the factored fatigue force determined above is converted to stress and compared to the resistance below in the subsequent section.

Resistance factor: $\phi_f := 1.0$

Factored fatigue resistance: $\Delta F_r := \phi_f \cdot \Delta F_n = 2.61 \ ksi$

Final Design Check

As outlined previously, a strength and fatigue limit state design check are to be made. The calculations herein compile the factored design loads and factored resistances computed in previous sections of the calculation set. Note that Fatigue II design checks are made in terms of stress. As such, the previously determined fatigue forces are converted to axial stress by considering shear lag effects in accordance with Table 6.6.1.2.3-1 (Section 7.2). Although not explicitly demonstrated, similar design calculations must be made for the connections and connecting parts.

Strength Limit State

Factored compression resistance: $P_{r.str} = 28.8 \ kip$

Governing factored force: $P_{str} = 26.4 \ kip$ (Compression)

$$Check := \left\| \begin{array}{l} \text{if } P_{r.str} \ge P_{str} \\ \quad \| \text{“OK”} \\ \text{else} \\ \quad \| \text{“N.G.; Refine Design”} \end{array} \right\| = \text{“OK”}$$

Fatigue Limit State

Factored fatigue resistance: $\Delta F_r = 2.61\ ksi$

Governing factored force: $P_{f2} = 0.9\ kip$

Assumed weld length: $L_w := 6\ in$

Distance from single-angle centroid to surface of gusset: $x_{bar} := 1.11\ in$

Shear lag factor: $U := 1 - \frac{x_{bar}}{L_w} = 0.8$

Net effective area: $A_{net} := U \cdot A_g = 1.96\ in^2$

Governing factored stress range: $\Delta f := \frac{P_{f2}}{A_{net}} = 0.44\ ksi$

$$Check := \left\| \begin{array}{l} \text{if } \Delta F_r \geq \Delta f \\ \quad \| \text{“OK”} \\ \text{else} \\ \quad \| \text{“N.G.; Refine Design”} \end{array} \right\| = \text{“OK”}$$

It is apparent that load-induced fatigue is not a concern for this cross-frame member of interest, as anticipated for this straight and normal bridge. These results are consistent with the major findings of NCHRP 12-113, which established geometric skew and curvature limits for when refined analysis is required to obtain live load force effects in cross-frames.

The design check for the strength limit state is also satisfied, which indicates that the assumed L4x4x5/16 single angle is adequate. Recall that the required strength was governed by the construction condition, which was dominated by stability bracing force effects. This indicates that stability bracing is an important design consideration, particularly in straight bridges where other load cases (e.g., dead load) tend to be less significant.

Stability Bracing - Stiffness

As outlined above and in proposed Article 6.7.4.2.2, braces must be designed to possess adequate strength and stiffness. The strength requirements were previously outlined. In this section, a separate check is provided to evaluate the required stiffness of the cross-frame. Similar to the brace strength requirements, proposed modifications have been made to the 15th Edition AISC provisions on torsional brace design. The proposed expression for the required brace stiffness is given with the following expression:

$$\beta_{T.req} := \frac{3.6\ L}{\phi_{br} \cdot n \cdot E \cdot I_{y.eff}} \cdot \left(\frac{\gamma_{CL} \cdot M_r}{C_b} \right)^2$$

As previously discussed, Liu et al. (2020b) observed that providing three times the ideal stiffness is more appropriate for beam buckling than twice the ideal stiffness, as assumed in the AISC bracing provisions. As such, the AISC equation has been modified by increasing the constant in the numerator by 50% (from 2.4 to 3.6). The following parameters describe the load and resistance factors assumed. Because the braces are evaluated during the critical stage of construction, the load factor associated with the construction condition is adopted here. The resistance factor is taken to match the values provided in AISC Appendix 6.3.

Resistance factor: $\phi_{br} := 0.80$

Load factor: $\gamma_{CL} := 1.4$

Recall the maximum DC1 moment as well as the moment gradient assumption from the brace strength calculation was governed by the positive moment region. As such, these parameters are established again.

Maximum unfactored moment: $M_r := 738\ kip \cdot ft$

Moment gradient factor: $C_b := 1.0$

The following parameters describe the cross-section of the girder and the bracing scheme. The girder is nonprismatic, which complicates the buckling behavior. Because the critical brace frames into the "small" section of the nonprismatic beam, those cross-sectional dimensions are conservatively assumed. The distance between the extreme fibers and the neutral axis is computed to determine an effective weak-axis moment of inertia, given that the section is also singly-symmetric.

Number of intermediate braces: $n_b = 4$

Tension flange width: $b_{f.t} := 16\ in$

Tension flange thickness: $t_{f.t} := 1.25\ in$

Compression flange width: $b_{f.c} := 14\ in$

Compression flange thickness: $t_{f.c} := 0.75\ in$

Web depth: $d_w := 42\ in$

Web thickness: $t_w := 0.4375\ in$

Distance from top fiber to neutral axis:

$$c := \frac{b_{f.t} \cdot t_{f.t} \cdot \frac{t_{f.t}}{2} + d_w \cdot t_w \cdot \left(t_{f.t} + \frac{d_w}{2}\right) + b_{f.c} \cdot t_{f.c} \cdot \left(t_{f.t} + d_w + \frac{t_{f.c}}{2}\right)}{b_{f.t} \cdot t_{f.t} + d_w \cdot t_w + b_{f.c} \cdot t_{f.c}} = 18\ in$$

Distance from bottom fiber to neutral axis: $t := \left(t_{f.t} + d_w + t_{f.c}\right) - c = 26\ in$

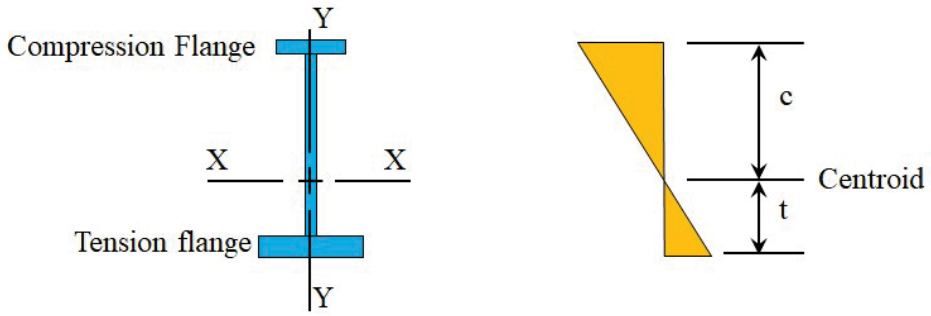

Figure 8: Schematic showing the definition of *c* and *t* variables

Tension flange moment of inertia: $I_{y.t} := \frac{1}{12} \cdot t_{f.t} \cdot {b_{f.t}}^3 = 426.7\ in^4$

Compression flange moment of inertia: $I_{y.c} := \frac{1}{12} \cdot t_{f.c} \cdot {b_{f.c}}^3 = 171.5\ in^4$

Effective moment of inertia: $I_{y.eff} := I_{y.c} + \left(\frac{t}{c}\right) \cdot I_{y.t} = 788.2\ in^4$

Therefore, the required torsional stiffness of the cross-frame is given as:

$$\beta_{T.req} := \frac{3.6\ L}{\phi_{br} \cdot n_b \cdot E \cdot I_{y.eff}} \cdot \left(\frac{\gamma_{CL} \cdot M_r}{C_b} \right)^2 = 8171\ \frac{kip \cdot in}{rad}$$

Now that the required stiffness has been established, the next step is to estimate the actual stiffness of cross-frame and verify its adequacy. As outlined extensively in Yura (2001) and the proposed Article 6.7.4.2.2, the torsional stiffness of a cross-frame must consider the effects of not only the brace itself, but also the effects of web distortion, in-plane girder, and its connections. The calculations herein evaluate each component of stiffness and then consider the combined effects against the required stiffness.

First, the stiffness of the brace is evaluated. The torsional stiffness of a K-type cross-frame can be estimated as the following expression (Yura, 2001):

$$\beta_b := R_{con} \cdot \left(\frac{2\ E \cdot {s_g}^2\ {h_b}^2}{\frac{8\ {L_d}^3}{A_d} + \frac{{s_g}^3}{A_s}} \right)$$

To solve for the torsional brace stiffness, several variables related to the cross-frame proportions must be established. Many of these variables have been previously defined but are presented again for reference. Note that the area of the strut and diagonal members of the cross-frame are identical (L4x4x5/16 single angle members).

Another important aspect is the inherent flexibility with the eccentric end connections of the cross-frame members. The connection stiffness is typically considered by assigning a modification factor to the stiffness of the brace. As highlighted previously, AASHTO LRFD recommends using a modification factor (R-factor) of 0.65 when evaluating cross-frames for stability-related applications. As such, that value is used here.

Modulus of elasticity, steel:	$E = 29000\ ksi$
Girder spacing:	$s_g := 120\ in$
Height of cross-frame brace:	$h_b = 30\ in$
Diagonal area:	$A_d := A_g = 2.4\ in^2$
Strut area:	$A_s := A_g = 2.4\ in^2$
Length of diagonal:	$L_d := \sqrt{\left(0.5 \cdot s_g\right)^2 + {h_b}^2} = 67.1\ in$
Stability modification factor (construction):	$R_{con} := 0.65$

Therefore, the torsional stiffness of the K-type cross-frame is given by the following, when considering the inherent flexibility of the connections:

$$\beta_b := R_{con} \cdot \left(\frac{2\ E \cdot {s_g}^2\ {h_b}^2}{\frac{8\ {L_d}^3}{A_d} + \frac{{s_g}^3}{A_s}} \right) = 283040\ \frac{kip \cdot in}{rad}$$

Note that the actual stiffness of the cross-frame is considerably larger than the required stiffness for the system; however, the brace stiffness is only one component of the total stiffness. As such, other components (i.e., cross-sectional distortion and in-plane girder effects) are considered herein. The total stiffness is then solved using the expression for springs in series.

With that in mind, the web-distortional effects are considered based on expressions developed by Yura

(2001). Note that web-distortional effects are generally only critical when a shallow brace is used relative to the girder depth and partial-depth stiffeners are used; this is most common when diaphragm beams are used as braces rather than cross-frames. Cross-frames, like the ones used in this design example, typically brace the full depth of the girder web. In this scenario, a 3-inch gap is assumed between the edge of the gusset plates and the inside face of top and bottom flanges. As such, web distortional effects are expected to be negligible; for the sake of completeness, a full calculation is presented below.

The following parameters characterize the dimensions of the cross-frames and connection plate stiffeners. A separate stiffness is evaluated for the top clear distance and the bottom clear distance as noted in proposed Article 6.7.4.2.2. Ultimately, the web distortion stiffness is the combined effect of both contributions.

Flange centroidal distance:	$h_o := 43\ in$
Clear distance outside brace:	$h_i := 3\ in$
Stiffener thickness:	$t_s := 0.5\ in$
Stiffener width:	$b_s := 12\ in$
Web thickness:	$t_w = 0.438\ in$

Therefore, the web distortional stiffness is computed as follows. Note that the value is orders of magnitude higher than the brace stiffness, as expected.

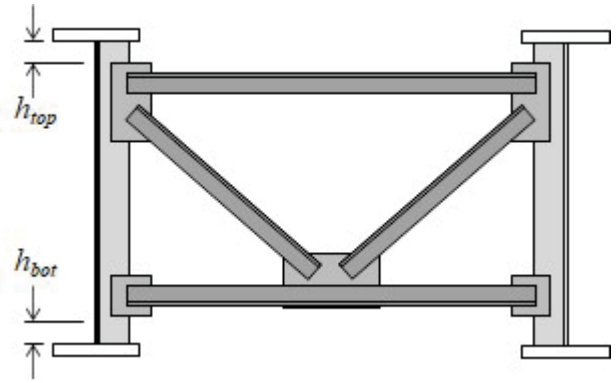

Figure 9: Schematic showing the definition of important cross-sectional distortion variables

$$\beta_{top} := \frac{3.3\ E}{h_i} \cdot \left(\frac{h_o}{h_i}\right)^2 \cdot \left(\frac{1.5\ h_i \cdot {t_w}^3}{12} + \frac{t_s \cdot {b_s}^3}{12}\right) = \left(4.72 \cdot 10^8\right)\ \frac{kip \cdot in}{rad}$$

$$\beta_{bot} := \beta_{top} = \left(4.72 \cdot 10^8\right)\ \frac{kip \cdot in}{rad}$$

$$\beta_{sec} := \frac{1}{\left(\frac{1}{\beta_{top}} + \frac{1}{\beta_{bot}}\right)} = \left(2.36 \cdot 10^8\right)\ \frac{kip \cdot in}{rad}$$

Lastly, the in-plane girder stiffness is computed. The in-plane girder stiffness is generally only critical for narrow superstructures with two or three girders across the width. For redundant systems with significant bridge width, the in-plane stiffness is general much larger than the brace stiffness. The following parameters describe the general layout of the framing plan. Note that the moment of inertia was previously computed in the original SBDH example.

Number of girders:	$n_g := 4$
Moment of inertia about x-axis:	$I_x := 15969\ in^4$

Span length: $L = 90\ ft$

Therefore, the in-plane girder stiffness is computed as follows. Note that the value is similar to that of the brace stiffness, given that the span is relatively narrow, but not enough to warrant serious consideration for system buckling effectives in Article 6.10.3.4.2 (Yura, 2008; Han and Helwig, 2020).

$$N_g := \frac{24\ (n_g - 1)^2}{n_g} = 54$$

$$\beta_g := \frac{N_g\ s_g^{\ 2}\ E \cdot I_x}{L^3} = 285865\ \frac{kip \cdot in}{rad}$$

The total, combined effect of each component is considered through a "spring in series" analogy. Note that the total stiffness is always less than the smallest of the three individual stiffness components. Given that full depth web stiffeners and a deep cross-frame was used in this example, the inverse of the cross-sectional distortion term is extremely small. Had this term been neglected altogether, as permitted in the proposed AASHTO *LRFD* Article 6.7.4.2.2, the system stiffness would be nearly identical to what is shown below.

$$\beta_T := \frac{1}{\left(\frac{1}{\beta_b} + \frac{1}{\beta_{sec}} + \frac{1}{\beta_g}\right)} = 142137\ \frac{kip \cdot in}{rad}$$

Finally, the total brace stiffness is evaluated against the required stiffness as shown in the calculations below:

Total stiffness: $\beta_T = 142137\ \frac{kip \cdot in}{rad}$

Required stiffness: $\beta_{T.req} = 8171\ \frac{kip \cdot in}{rad}$

$$Check := \left\| \begin{array}{l} \text{if } \beta_T \geq \beta_{T.req} \\ \quad \| \text{“OK”} \\ \text{else} \\ \quad \| \text{“N.G.; Refine Design”} \end{array} \right\| = \text{“OK”}$$

The cross-frame panel comprised of L4x4x5/16 single-angle sections is adequate in terms of stability bracing stiffness by a large margin. Part of this is because the beam span is relatively small (90 feet) and because the cross-frames are relatively stiff elements. In general, designers will often find that typical details that are commonly used for cross-frames satisfy the bracing requirements.

References

American Association of State Highway and Transportation Officials. 2014. *G13.1 Guidelines for Steel Girder Bridge Analysis.* 2nd Ed.

American Association of State Highway and Transportation Officials. 2020. *LRFD Bridge Design Specifications.* 9th Ed. Washington, D.C.

American Institute of Steel Construction. 2010. *Specification for Structural Steel Buildings.* 14th Ed. Chicago, IL.

American Institute of Steel Construction. 2016. *Specification for Structural Steel Buildings.* 15th Ed. Chicago,

IL.

Barth, K. 2015. *Steel Bridge Design Handbook Design Example 2A: Two-Span Continuous Straight Composite Steel I-Girder Bridge.* Washington, DC: Federal Highway Administration.

Battistini, A., W. Wang, T. Helwig, M. Engelhardt, and K. Frank. 2016. "Stiffness Behavior of Cross Frame in Steel Bridge Systems." *Journal of Bridge Engineering* (American Society of Civil Engineers) 21 (6).

Han, L., and T. Helwig. 2020. Elastic Global Lateral Buckling of Straight I-Shaped Girder Systems." *Journal of Structural Engineering* (American Society of Civil Engineers) 146 (4).

Helwig, T., and Yura, J. 2015. *Steel Bridge Design Handbook: Bracing System Design*. Publication No. FHWA-HIF-16-002, Washington, DC: Federal Highway Administration.

Liu, Y., and T. Helwig. 2020a. "Torsional Brace Strength Requirements for Steel I-Girder Systems." *Journal of Bridge Engineering* (American Society of Civil Engineers) 146 (1).

Liu, Y., B. Kovesdi, and T. Helwig. 2020b. "Torsional Bracing Stiffness Requirements for Steel I-Girder Systems." *Journal of Structural Engineering* (American Society of Civil Engineers). [Under Revision]

Rivera, J., and B. Chavel. 2015. *Steel Bridge Design Handbook Design Example 3: Three-Span Continuous Horizontally Curved Composite Steel I-Girder Bridge.* Washington, DC: Federal Highway Administration.

White, D., D. Coletti, B. Chavel, A. Sanchez, C. Ozgur, J. Jimenez Chong, R. Leon, et al. 2012. *Guidelines for Analysis Methods and Construction Engineering of Curved and Skewed Steel Girder Bridges.* NCHRP Report 725, Washington, D.C.: Transportation Research Board.

White, D., T. Nguyen, D. Coletti, B. Chavel, M. Grubb, and C. Boring. 2015. *Guidelines for Reliable Fit-Up of Steel I-Girder Bridges.* NCHRP 20-07/Task 355, Washington, D.C.: Transportation Research Board, National Research Council.

Yura, J. 2001. "Fundamentals of Beam Bracing." *Engineering Journal* (American Institute of Steel Construction) 11-26.

Yura, J., T. Helwig, R. Herman, and C. Zhou. 2008. "Global Lateral Buckling of I-Shaped Girder Systems." *Journal of Structural Engineering* (American Institute of Steel Construction) 134 (9).